Journal of Biomolecular NMR (2018) 70:123–131
https://doi.org/10.1007/s10858-018-0164-7

ARTICLE

Whole cell solid-state NMR study of *Chlamydomonas reinhardtii* microalgae

Alexandre A. Arnold[1] · Jean-Philippe Bourgouin[1] · Bertrand Genard[1,2] · Dror E. Warschawski[1,3] · Réjean Tremblay[2] · Isabelle Marcotte[1]

Received: 29 October 2017 / Accepted: 4 January 2018 / Published online: 11 January 2018

Abstract

In vivo or *whole-cell* solid-state NMR is an emerging field which faces tremendous challenges. In most cases, cell biochemistry does not allow the labelling of specific molecules and an in vivo study is thus hindered by the inherent difficulty of identifying, among a formidable number of resonances, those arising from a given molecule. In this work we examined the possibility of studying, by solid-state NMR, the model organism *Chlamydomonas reinhardtii* fully and non-specifically ^{13}C labelled. The extension of NMR-based dynamic filtering from one-dimensional to two-dimensional experiments enabled an enhanced selectivity which facilitated the assignment of cell constituents. The number of resonances detected with these robust and broadly applicable experiments appears to be surprisingly sparse. Various constituents, notably galactolipids abundant in organelle membranes, carbohydrates from the cell wall, and starch from storage grains could be unambiguously assigned. Moreover, the dominant crystal form of starch could be determined in situ. This work illustrates the feasibility and caveats of using solid-state NMR to study intact non-specifically ^{13}C labelled micro-organisms.

Keywords In vivo NMR · Magic-angle spinning · Lipids · Cell-wall · Starch · Isotope labelling · Dynamic filters

Introduction

Standing at the basis of the aquatic food chain, microalgae are of capital importance to their ecosystem. The key role that they play also makes them excellent sentinel species which report on the health of their milieu. In addition, their ability to photosynthetically transform CO_2 into lipids has sparked a growing interest in their use as a sustainable source of biofuel which simultaneously reduces atmospheric CO_2 (Wijffels and Barbosa 2010). Furthermore, microalgae can also produce high-value nutrients such as carotenoids and omega-3 fatty acids, as well as food products in the form of proteins and starch (Wijffels and Barbosa 2010). The possibility of using microalgae for recombinant protein production has also been explored, and examples include overexpression of antibodies against the simplex herpes virus or an anthrax protective antigen (Specht et al. 2010). These biotechnological applications hold a huge economic and environmental impact. They however face important technical difficulties, for example oil production and purification or recombinant protein overexpression yields all need to be optimized. All these processes would greatly benefit from a better characterization of the part played by each molecule in the cell and the influence of growth conditions on their abundances. Therefore analytical techniques are required to better identify those molecules and understand molecular changes in microalgae, especially under bioengineering conditions, or when exposed to contaminants.

Among the techniques used to study microalgae, solid-state NMR is a new promising approach to characterize whole cells in vivo (Arnold et al. 2015; Warnet et al. 2015).

Electronic supplementary material The online version of this article (https://doi.org/10.1007/s10858-018-0164-7) contains supplementary material, which is available to authorized users.

✉ Isabelle Marcotte
marcotte.isabelle@uqam.ca

[1] Department of Chemistry, Université du Québec à Montréal, Downtown Station, P.O. Box 8888, Montreal H3C 3P8, Canada

[2] Institut des Sciences de la Mer de Rimouski, Université du Québec à Rimouski, 310 allée des Ursulines, Rimouski G5L 3A1, Canada

[3] Laboratoire de Biologie Physico-Chimique des Protéines Membranaires, UMR 7099, CNRS, Université Paris Diderot and IBPC, 13 rue Pierre et Marie-Curie, 75005 Paris, France

This method is non-destructive and non-invasive, and therefore alleviates the extraction steps usually required to analyze the microalgal content which can potentially induce chemical modifications. In our previous study, we showed that one-dimensional (1D) ^{13}C solid-state NMR with magic-angle spinning (MAS) of fully labeled microalgae could be used to evidence interspecies differences in cell wall constituents, storage sugars and membrane lipid composition. The objective of this work is to refine the identification and characterization of microalgal cell constituents using high-resolution 2D ^{13}C solid-state NMR. We have chosen whole *Chlamydomonas reinhardtii* cells, a well-established model system with numerous available mutant strains and whose genome is now fully established (Blaby et al. 2014; Merchant et al. 2007). *C. reinhardtii* is an egg-shaped freshwater green microalga, roughly 10 µm in size, which possesses two equal flagella (Hoek et al. 1995). Phylogenetic and phylogenic analyses reveal that it shares features with non-chlorophyte algae and land plants, but also with mammals (Blaby et al. 2014; Merchant et al. 2007). It is used for the study of a wide spectrum of processes from photosynthesis to biofuel production (Blaby et al. 2014). It can be notably grown autotrophically under UV light, or heterotrophically in the dark (Hoek et al. 1995). Among its particularities, it has only one chloroplast and its cell wall is made of multi-layered hydroxyproline-rich glycoproteins without cellulose (Hoek et al. 1995).

To achieve selectivity in such complex biological system, we exploit different NMR experiments exploring the variety of dynamical regions found in microalgae (Arnold et al. 2015). We first present the results of polarization transfer methods which are sensitive to dynamics on whole microalgae, following our previous work (Arnold et al. 2015). An improvement in resolution and spectral simplification is obtained by extending this dynamical selectivity during the mixing time of a 2D spectrum. Using these experiments we identify the main constituents in a whole microorganism in situ. More specifically, galactolipids which are abundant in the organelles' membranes are assigned, as is starch—the major storage sugar—and characteristic glycans from the microalgal cell wall. Notably, the anomeric resonances of the latter can be distinguished downfield from those of starch and galactolipids. The principal advantages and necessary improvements of this approach to whole-cell NMR are discussed.

Materials and methods

Materials

^{13}C labelled sodium bicarbonate was obtained from Cambridge Isotope Laboratories (Tewksbury, MA, USA). All chemicals used for the growth medium, natural-abundance corn starch and Percoll used for purification were obtained from Sigma-Aldrich (Oakville, ON, Canada). *C. reinhardtii* wild type strain 222+ was obtained from the collection of the Institut de Biologie Physico-Chimique (Paris, France).

Cell growth conditions and starch extraction

Chlamydomonas reinhardtii was cultivated as previously described (Arnold et al. 2015). In short, the culture medium was supplemented with $NaH^{13}CO_3$ to a final concentration of 0.1% (w/v). The culture system was then sealed and the medium was purged with nitrogen gas to eliminate atmospheric CO_2. The culture was allowed to grow at a temperature of 23 °C for 5 days under constant gentle shaking and a continuous illumination until the plateau region of the growth curve. A more detailed description of the growth conditions is given in the supplementary material. The algae were mildly centrifuged ($< 3000\times g$) and the pellet manually transferred to the NMR rotor using a spatula. Mild centrifugation conditions are required to preserve the integrity of the cells. The approximate yield is 160 mg of microalgae (dry mass) per liter of culture. The 4 mm rotors contained roughly 100 mg of hydrated algae while the 1.9 mm contained 15 mg. Samples are 15% algae and 85% buffer by weight.

We adapted the protocols of starch extraction from Buléon et al. (1997). Cells were centrifuged 8 min at $1600\times g$, rinsed twice with 10 mM Tris HCl at pH 8, then re-centrifuged. They were diluted with the same buffer at a concentration of 10^8 cell/ml and then lysed by sonication. The lysate was centrifuged 15 min at $2000\times g$ at 5 °C. The supernatant was removed and the pellet re-suspended into one volume of buffer for another cycle of sonication and centrifugation. The pellet was re-suspended in one volume of buffer, added gently to five volumes of Percoll (colloidal silica particles of 15–30 nm diameter coated with PVP), and centrifuged again. This procedure was repeated and the final pellet was rinsed twice with milli-q water at 4 °C, before being freeze-dryed.

Solid-state NMR

All spectra were recorded with a Bruker Avance III-HD (Milton, ON, Canada) using either a double resonance 4 mm or a triple resonance 1.9 mm MAS probe used in double resonance mode. The larger 4 mm rotors were favored for experiments which do not require high spinning frequencies to improve signal to noise. The spinning speed was fixed to 10 kHz for standard one-dimension and dipolar based 2D experiments [dipolar-assisted rotational resonance (DARR) and proton-driven spin diffusion (PDSD)]. Radio-frequency fields of 75 and 85 kHz were applied on the ^{13}C and ^{1}H

channels respectively (corresponding to 3.3 and 2.9 µs long 90° pulses). The ^{1}H radiofrequency amplitude was ramped from 70 to 100% during cross-polarization (CP) and spinal-64 decoupling was used during acquisition in all spectra. The delays in the refocused INEPT steps were 1.78 ms. For the *J*-coupling based TOBSY (Total through bond correlation spectroscopy) experiments performed on the 1.9 mm probe, the spinning frequency was fixed at 26.667 kHz and the applied radio-frequency fields were of 85 and 100 kHz for ^{13}C and ^{1}H channels respectively (corresponding to 2.9 and 2.5 µs long 90° pulses). The maximum TOBSY mixing time which could be attained without probe arcing was 6.75 ms. Spectra were recorded at 298 K.

Results and discussion

Achieving selectivity in fully labelled whole cells

The challenge of studying fully ^{13}C labelled intact cells consists in achieving signal selectivity to facilitate peak assignment. As shown in our previous work, it is possible to considerably simplify the 1D spectra of fully ^{13}C-labelled whole microalgal cells by exploiting the dependency of NMR interactions on internal dynamics (Arnold et al. 2015). Indeed, while rigid segments will be favored by NMR methods which rely on dipolar couplings, a high mobility will average out these interactions, thus *J*-coupling based techniques will have to be used. Note that this approach has been used for the study of large membrane protein complexes (Andronesi et al. 2005) or amyloid fibrils (Siemer et al. 2006) and has also been applied to the study of cellular envelopes of *Escherichia coli* (Renault et al. 2012), however never, to our knowledge, of whole organisms.

A 1D experiment can be initiated by a dipolar-based polarization transfer (cross-polarization, CP) or a *J*-couple mediated transfer (INEPT). In addition, a ^{1}H–^{13}C polarization transfer can be achieved by heteronuclear NOE. Although this procedure will enhance rigid and mobile moieties, the latter will be slightly favored (Warschawski and Devaux 2000). As can be expected for a whole cell which presents a strong dynamical heterogeneity, the NOE transfer results in the best overall enhancement (however with poor selectivity). Figure 1 shows the ^{13}C spectra of whole microalgal cells obtained by these three selective polarization transfer methods. In principle, highly dynamic vs. rigid molecules should have different relaxation properties. However, according to our ^{13}C T_1 measurements (not shown), relaxation times in *C. reinhardtii* range between 0.5 and 1.75 s and differences are therefore rather small. Nevertheless, in an attempt to further filter the 1D spectra, we added a 1 s delay during which ^{13}C magnetization is stored along the z axis and ^{13}C longitudinal relaxation can take place

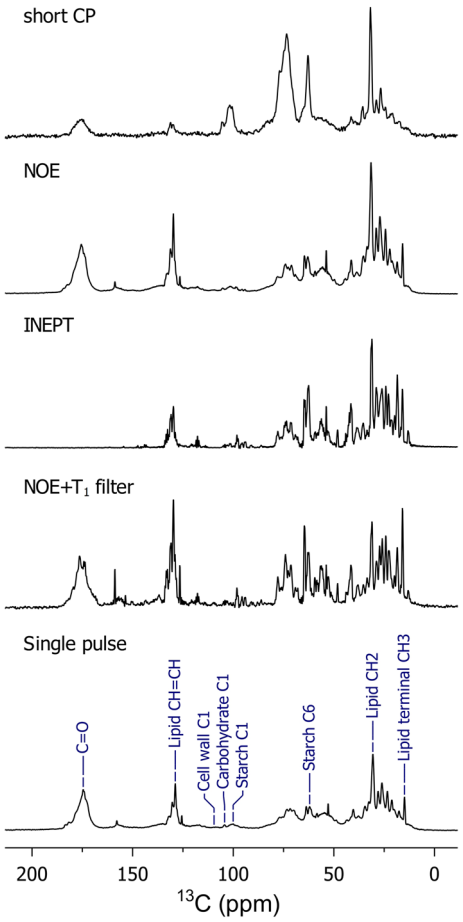

Fig. 1 Dynamically-filtered 1D ^{13}C solid-state NMR spectra of *Chlamydomonas reinhardtii* microalgae. Spectra obtained using (*a*) 0.75 ms-long CP and high power decoupling, (*b*) low-power NOE enhancement and high power decoupling, (*c*) INEPT polarization and low-power GARP decoupling, (*d*) low-power NOE enhancement, 1 s of T_1 filter and low power decoupling and (*e*) quantitative spectrum with standard excitation (90° pulse), high power decoupling and 15 s recycle delay

(Fig. 1d). The dynamic selectivity is most notably apparent in the INEPT and T_1-filtered spectra (1C and 1D) where the sharpest peaks, which are found in the aliphatic (0–50 ppm) and double bond regions (~ 130 ppm), are enhanced. Interestingly, sharp peaks are also found between 50 and 70 ppm, suggesting that mobile carbohydrates are also present which can be assigned to galactolipids or cell wall glycans (vide infra). The CP spectrum (Fig. 1a) is dominated by a small number of broad lines in the carbohydrate region. In addition to them, the most intense peaks of the non-selective direct excitation spectrum (Fig. 1e) are also present on the CP spectra, although strongly attenuated. A good selection of rigid segments can therefore be obtained using CP, although it is not complete in a 1D spectrum.

We previously reported a tentative assignment of microalgal cell constituents using some of these simplified 1D

spectra (Arnold et al. 2015). However, a more definitive assignment can only be established using 2D experiments which second dimension improves the resolution, while the mixing step can enable a second dynamics selectivity filter for rigid components. Indeed, a dipolar-coupling based mixing such as PDSD or DARR will further select rigid segments while a TOBSY-type mixing, which relies on *J*-couplings, will be equally efficient for mobile or rigid molecules. Finally during the detection, applying a weak GARP sequence will only sufficiently decouple protons in highly dynamic regions whereas a strong decoupling such as TPPM or Spinal-64 will be needed for the rigid domains. Additional selectivity can thus be obtained during the spectrum acquisition. In principle, longitudinal relaxation times should also enable an additional dynamical sorting (as shown in the T_1 filtered 1D experiments). However, since T_1 values are not very different in our samples, a complete filtering is not possible and we privilege a long enough recycle delay to improve signal to noise.

Figure 2 shows the complete ^{13}C–^{13}C correlation spectra favoring molecular segments with low (blue) or high (red) mobility. Close observation reveals that a majority of cross peaks are exclusively found in one or the other spectrum, with very little overlap. Indeed, in addition to the gain in resolution due to the second dimension, the selectivity is further optimized from the 1D spectra thanks to the dynamically sensitive mixing scheme. It is also interesting to note

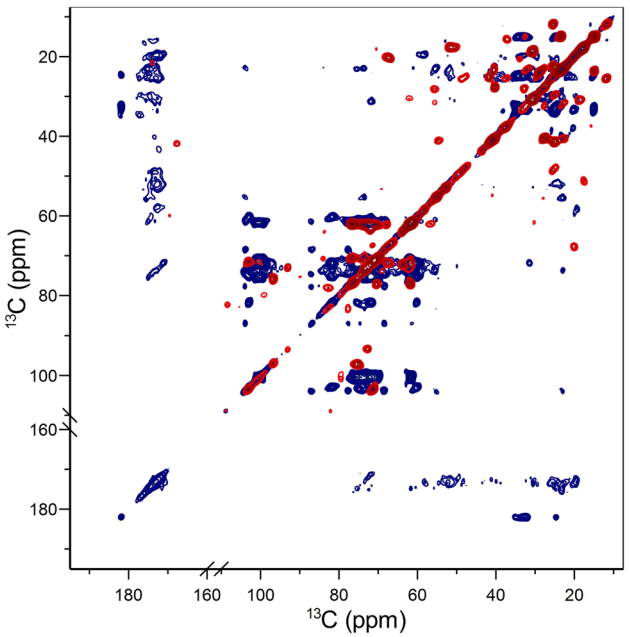

Fig. 2 Dynamically-filtered 2D ^{13}C solid-state NMR spectra of whole *C. reinhardtii* microalgae. Rigid consitutents (in blue) are detected using 0.75 ms CP and 150 ms DARR while mobile constituents (in red) are detected using a RINEPT polarization and 6.75 ms *J*-coupling mediated TOBSY

the relative paucity of peaks on both spectra considering that a whole microorganism is being monitored. A consequence of the selectivity filters—combined to the relatively weak sensitivity of solid-state NMR—is thus to simplify the spectra which are now dominated by the major constituents of the cells, namely membrane lipids, storage sugars and proteins, consistent with the proportions of carbohydrates, lipids and proteins in *C. reinhardtii* which can be found in Supplementary Information Fig. SI1.

In the following sections, dynamical signal filtering will be exploited to identify the constituents of important cell compartments in *C. reinhardtii*. More specifically we will investigate the cell wall (the first barrier crossed or targeted by contaminants), membrane lipids (where the latter can accumulate) and starch grains which are essential for the energy storage of this microalga.

Identification of cell constituents: membrane and storage lipids

Lipids in microalgae can be separated in two main categories according to their polarity (Guschina and Harwood 2009). The membrane-forming polar lipids mainly play a structural role in organelle compartmentalization. Among them, the most abundant for *C. reinhardtii* are the glycosylglycerides also known as galactolipids such as monogalactosyl diacylglyceride (MGDG 38%), digalactosyl diacylglyceride (DGDG 24%) and sulfoquinovosyl diacylglycerol (SQDG 12%) (Vieler et al. 2007). All lipid structures are displayed in Fig. SI2. Glycosylglycerides are essentially found in photosynthetic chloroplast and thylakoid membranes. Less abundant are betaine lipid diacylglyceryl-trimethylhomoserine (DGTS 12%) and phospholipids, essentially phosphatidylglycerol (PG 10%) and phosphatidylethanolamine (PE 3%) (Arnold et al. 2015). In addition to these membrane-forming lipids *C. reinhardtii* produces non-polar storage lipids, i.e. triacylglycerols (TAGs), which accumulate as droplets in both the plastids and the cytosol (Guschina and Harwood 2009). Under certain stress conditions *C. reinhardtii* has been shown to accumulate significant amounts of TAGs, to the extent of virtually filling the whole cell (Merchant et al. 2012).

Both structural and storage lipids are highly mobile and dipolar-mediated experiments are reported to be only weakly efficient in membranes (Warschawski and Devaux 2000). We therefore exploited the *J*-coupling mediated RINEPT-TOBSY experiment of which the carbohydrate region of the spectrum is shown in Fig. 3. Single quantum double quantum correlation experiments such as INADEQUATE could be an interesting alternative to resolve the poorly dispersed carbohydrate spectra (Dick-Perez et al. 2011; Rondeau-Mouro et al. 2006). This experiment also uses *J*-couplings and could therefore be amenable to study mobile molecules.

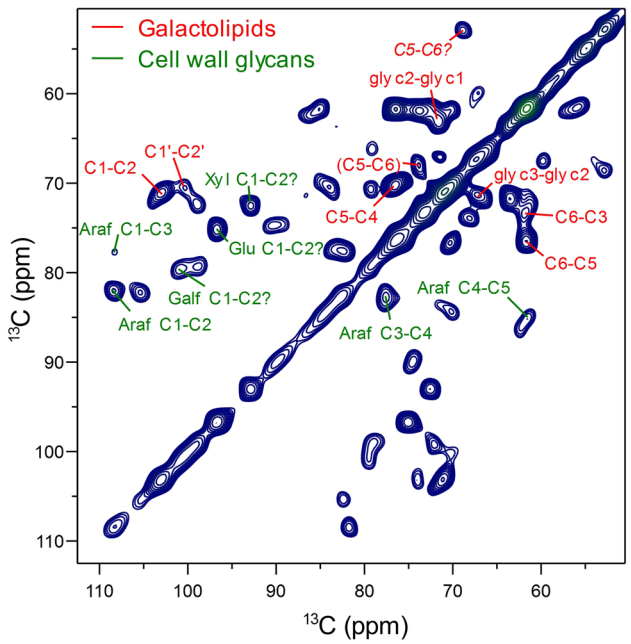

Fig. 3 ^{13}C RINEPT-TOBSY spectrum with 4.5 ms mixing time showing correlations between carbons of mobile molecules in whole *C. reinhardtii* cells. Assignments of lipids are shown in red, cell wall resonances in green. The prime symbol indicates carbons in the first galactosyl group of DGDG, carbons in the terminal galactosyl group of DGDG are between parentheses and the tentative SQDG assignment is in italic

However, we favored the TOBSY experiment which produces symmetric spectra such as the rigid-sensitive CP-DARR, thus facilitating their comparison.

The most abundant galactolipids are MGDG and DGDG. Since the single galactosyl group of MGDG and the first one of DGDG have almost identical C1 to C4 chemical shifts, their signals were therefore expected to be readily visible (Johns et al. 1977). As shown in Fig. 3, a spin system with chemical shifts at (103.2-71.1-73.5-70.2 ppm) can be assigned to the "identical" galactosyl groups of these two lipids. The C5 and C6 positions of the galactosyl group which differ between the two lipids can be assigned to (76.5–61.8 ppm) for MGDG, and (74.0–68.1 ppm) for DGDG (Johns et al. 1977). The cross peak between these positions corresponding to DGDG has a slightly lower intensity than the one of MGDG as expected from their relative abundances. The terminal galactosyl group of DGDG is reported to have poorly dispersed C2′ to C5′ carbons which all fall between 70.1 and 71.2 (Johns et al. 1977). Their correlations are thus most likely too close to the diagonal to be resolved. Interestingly, the diagonal crosspeak at this position is particularly intense. A weaker peak at (100.2–70.3 ppm) can however reasonably be assigned as the C1′–C2′ cross peak of the second galactosyl group in DGDG. Finally, the C5–C6 pair which should fall at 71.2–62.3 ppm according to the literature is likely to be hidden by the intense glycerol backbone cross peaks (67.1-71.5-63.3 ppm) also shown in Fig. 3. Experimental and literature values are summarized in Table SI1.

Note that it is not possible with our experimental resolution to distinguish the backbone glycerol moieties from the different lipids present, due to their small dispersion (see the literature values in Table SI1). The remaining lipids SQDG, DGTS and PG could not be detected since they are most likely below our detection limit. In addition, their resonances are expected to at least partially overlap with those of the more abundant galactolipids. According to the literature (Johns et al. 1978), the C5–C6 correlation of SQDG (71.7, 54.3 ppm) should in principle stand out; however, a single resonance at (68.8, 52.9 ppm) could be found in this region which we can only very tentatively assign to SQDG.

After identification of the main *C. reinhardtii* lipids MGDG and DGDG from the carbohydrate region of the mobile-sensitive spectrum, we analyzed the aliphatic region (0–50 ppm) which is crowded with peaks from all lipids (polar and non-polar), proteins' mobile regions, and potentially even pigments (see Fig. SI4). Nevertheless, this region informs on the lipid chains, and intense correlations between 14.5 and 14.8 and 21.1–23.4 ppm most likely correspond to the terminal methyl and the adjacent methylene group in the lipid acyl chains. The cross peak at 32.5/23.2 ppm is probably the methylene group adjacent to a methylene bonded to a methine group. A strong cross peak is also observed between a lipid methylene group at 26 ppm which is intercalated between two double bonds at 128 ppm.

Under the growth conditions used in this work, the storage of TAG is not favored; therefore this lipid is not expected to be present in large proportions. TAG chemical shifts have a very strong overlap with those of other lipids, and cannot be easily isolated in our spectra (Beal et al. 2010). It has been shown that growing *C. reinhardtii* in a nitrogen-depleted medium enhances the production of TAGs (Merchant et al. 2012; Siaut et al. 2011). It would be of interest to grow the microalgae in these conditions in an attempt to better identify the presence of TAGs.

Pigments are also included in the lipid fraction of microalgae. The main pigments present in *C. reinhardtii* are chlorophylls *a* and *b* and β-carotene (Hoek et al. 1995), which respectively account for 45, 20 and 18 mol % of all pigments (Bonente et al. 2012). The remaining proportion corresponds to other minor pigments lutein, violaxanthin, neoxanthin, zeaxanthin, antheraxanthin, siphonein and siphonoxanthin (Hoek et al. 1995; Bonente et al. 2012). Despite the functional importance of pigments, their relative abundance is very low (on the order of µg/mg by dry weight of microalgae). As part of complexes formed with photosystems within thylakoid membranes, their dynamic is likely to be intermediate or slow. Chlorophyll *a* in particular has been

well characterized by ^{13}C NMR even in its aggregated form (Boender et al. 1995). The central chelating complex of chlorophyll should show correlation peaks between (140–160 ppm) and (90–110 ppm)—an unusual region for proteins, carbohydrates and lipids. This area is devoid of peaks in all our spectra, revealing that pigments' signals fall below our present detection limit for whole cells, or cannot be detected when signals from dynamic constituents are selected.

Identification of cell constituents: cell wall

Unlike in cellulose-forming microalgae or higher plants (Dick-Perez et al. 2011; Wang and Hong 2016), the cell wall of *C. reinhardtii* is composed of fibrous hydroxyproline-rich glycoproteins (Hoek et al. 1995). The glycosyl groups found in the sidechains are reported to be mainly galactose (46%) and arabinose (41%), the remaining minor constituents being glucose (8%), xylose (4%) and mannose (1%) (Ferris et al. 2001). These carbohydrates form complex linear and branched *O*-glycan sidechains composed of both pentoses and hexoses with occasional methylations (Bollig et al. 2007; Kilz et al. 2000). Four short linear O-glycans extracted from *C. reinhardtii* have been analyzed in more detail and reported to be composed of galactose and arabinose in their furanose forms (Galf and Araf, respectively), with Araf linked to hydroxyproline (Bollig et al. 2007).

As revealed by electron microscopy, a cross-section of the cell wall shows a granular central region sandwiched between two layers of crystalline glycoproteins (Hoek et al. 1995). When fully hydrated, the dynamics of the cell wall is thus likely to be complex and cell wall resonances possibly visible in *both* rigid- and mobile-sensitive spectra. Indeed, the most accurate identification of the cell wall constituents comes from the analysis of the carbohydrate region (50–110 ppm) in both mobile- and rigid-sensitive experiments. The crystalline region should however only be present in dipolar-based spectra.

As shown in Fig. 3 on the RINEPT-TOBSY spectrum, the anomeric peak with higher frequency lies at 108.5 ppm which falls close to both Galf and Araf (Bradbury and Jenkins 1984). A spin system with chemical shifts (108.5, 81.9, 77.6, 83.0, 63.8 ppm) can be isolated in the mobile-sensitive spectrum, in good agreement with those assigned in the literature to α-Araf with chemical shifts (108.2, 82.0, 77.6, 82.5–84.9, 62.3–67.8 ppm) (Dick-Perez et al. 2011; Tan et al. 2004). Of these peaks, only the most intense C1–C2 correlation is weakly present on the dipolar-based DARR spectrum (Fig. 4), suggesting that this glycan is highly mobile and possibly assigned to a terminal residue (Tan et al. 2004). A moderately intense crosspeak at 105.2 ppm seems to show the same correlation pattern as the one at 108.5 ppm, therefore it is reasonable to also assign it to Araf with a

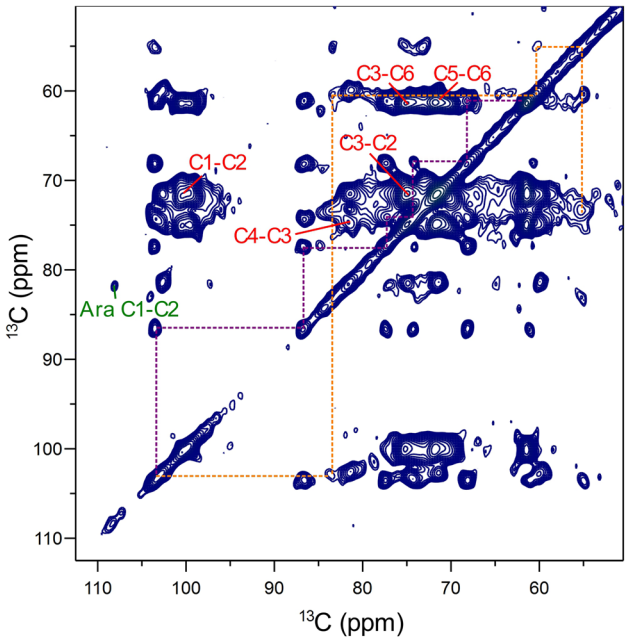

Fig. 4 ^{13}C CP-DARR spectrum with 100 ms mixing time showing correlations between rigid molecules in whole *C. reinhardtii* microalgae. Starch assignments are in red, cell wall constituents are shown in green. Connectivities between additional putative cell wall resonances are shown in purple and yellow

different type of linkage which would result in the different C1 chemical shift. At lower ppm values, two intense crosspeaks detected with chemical shifts (96.7–75.0 ppm) and (93.0–72.5 ppm) are in excellent agreement with the C1–C2 pairs respectively reported for β-glucose and α-xylose both in their pyranose form (Bradbury and Jenkins 1984). Unfortunately, no further correlations could be detected to confirm this assignment. One explanation for the absence of the additional correlations could be that at least parts of the cell wall would be in an intermediate motional regime where neither INEPT nor dipolar based transfers would be efficient. The remaining resonances at (100.7–79.6) (100.3–70.5) and (98.9–79.3) ppm fall close to those reported for the C1 carbons of Araf and Galf in Hyp-*O*-bound glycans extracted from *C. reinhardtii* (Bollig et al. 2007); however, only the C1 positions are reported and their firm assignment would need further data.

Figure 4 shows the dipolar-based CP-DARR spectrum of the same region. Readily identifiable are the crosspeaks from starch which will be described in the next section. In addition, strong correlations can be detected in two spin systems: one at (103.5, 86.8, 77.4, 74.4, 68.2, 61.1 ppm) and a second one at (103.5, 83.4, 75.1, 73.1, 60.5, 55.0 ppm). These spin systems could not be assigned to a single carbohydrate group and therefore probably result from a superposition of various glycans. The cell wall of *Chlamydomonas* is reported to be partially crystalline and very fast spin diffusion might

occur, leading to cross correlations between carbohydrates as opposed to within one carbohydrate. Their assignment is thus much difficult and the study of purified cell wall might be necessary to conveniently assign cell wall resonances in the whole organism. Nevertheless, the unusually high 87 ppm resonance suggests the presence of C2 or C4 glycosidic linkages. Similarly, the unusually low 55 ppm peak suggests the presence of C6 glycosidic linkages.

In situ characterization of starch

The main storage product of *C. reinhardtii* is starch which accumulates into grains within the chloroplast (Hoek et al. 1995). Starch is one of the most abundant biopolymers in nature. It is composed of varying amounts of amylopectin and amylose which can be in an amorphous form or found in two different crystalline double-helix forms noted A and B. It can also be found in the V form when bound to amylopectin for example. It is important to determine the structure and crystallinity of starch components as they determine its bioavailability for the microorganism and for its use in biotechnology.

By using a short 750 µs CP transfer followed by a 3 s long PDSD time, the only remaining resonances are those associated with crystalline starch (see Fig. 5). The assignment is unambiguous as demonstrated by superimposing the spectrum of ^{13}C-labelled starch extracted from *C. reinhardtii* cells. A one dimensional CP spectrum of the extracted starch can also be compared to a spectrum of natural abundance hydrated corn starch, which is reported to be close to *Chlamydomonas'* starch and crystallizes in the A form (Tang and Hills 2003). As can be seen in Fig. 5, these spectra are very similar.

The resolution provided by the 2D spectrum allows detecting three anomeric peaks with chemical shifts 102.7, 100.4 and 100.2 ppm, in good agreement with values reported in the literature for starch (Tang and Hills 2003). These three C1 resonances are usually associated to the presence of A-type amylose in the starch grains, in good agreement with results obtained by X-ray diffraction with *C. reinhardtii* (Buleon et al. 1997).

The smaller C1 peak at 102.7 ppm with the C4 peak at 81.3 ppm can be assigned to the amorphous regions (Tang and Hills 2003). The C2, C3, C6, peaks at 71.8, 75.2 and 61.7 ppm are in good agreement with those reported for B-type amylose (72.1, 75.1 and 61.3 ppm) (Rondeau-Mouro et al. 2006) but are also consistent with the A-type structure (Tang and Hills 2003). Here it should be specified that only one 2D solid-state NMR study has been published on starch. The work by Rondeau-Mouro et al. (2006) reports the values of all chemical shifts for B-type amylose; however, the complete C1–C6 assignment for other starch types is not known. An extensive 2D solid-state NMR study of the other forms of starch would be an important step forward in the study of this biopolymer. Nevertheless, our results show that the molecular structure of starch grains in microalgae can be probed in situ by solid-state NMR using the appropriate dynamic filter. They also show that starch storage in *C. reinhardtii* is crystalline and likely dominated by the A form.

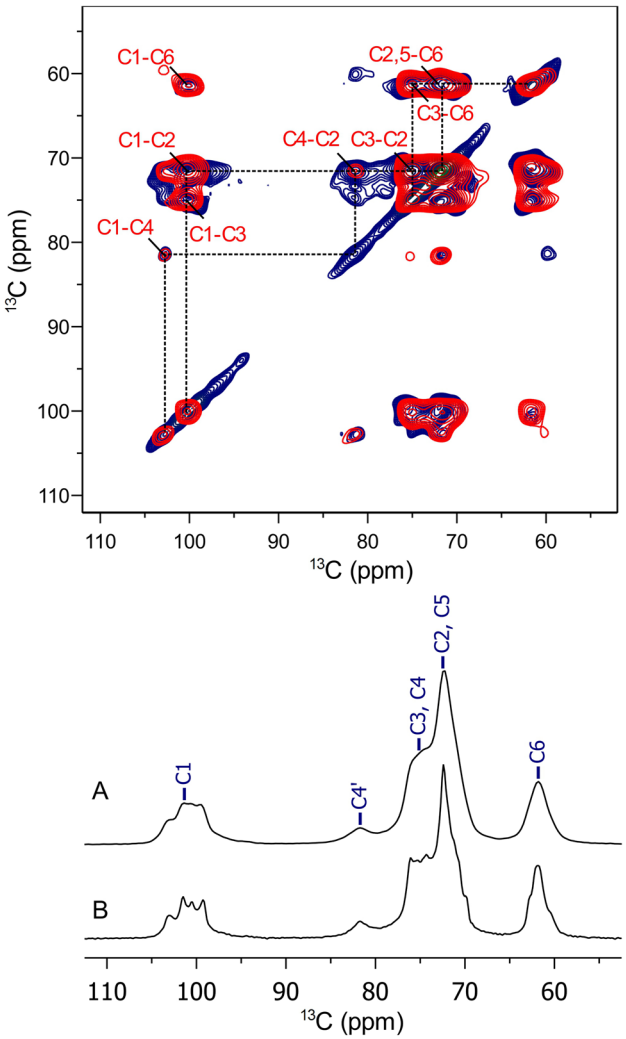

Fig. 5 ^{13}C CP—3 s PDSD spectrum of whole *C. reinhardtii* microalgae showing the characteristic peaks of starch (red) and CP—150 ms DARR spectrum of pure extracted starch (blue). (*A*) CP spectrum of extracted starch and (*B*) CP spectrum of natural-abundance corn starch

In search of other constituents: proteins, metabolites and degradation products

Proteins account for about 30% of the dry weight of *C. reinhardtii* grown in autotrophic conditions (Fig. SI1) and an important spectral contribution from proteins should thus be expected (Boyle and Morgan 2009). However, this spectral intensity will be distributed amongst the peaks

corresponding to the more than 15,000 proteins found in this microorganism's proteome (Merchant et al. 2007). The protein signal contribution can be roughly estimated by considering, on the 1D spectrum, the area of the broad carbonyl peaks. Considering one carbonyl per amino acid and two per lipid, and that proteins are approximately about 1.5 times more abundant than lipids (see the autotrophic condition in Fig. SI1), approximately 50% of the carbonyl peak resonance would correspond to amino acids. The intensity of the remaining amino acid peaks, distributed throughout all amino acid types, can be estimated to 1/20th of half the carbonyl's and therefore much lower than the carbohydrates and lipids' contribution. Still, unambiguous amino acid correlations can be found, but cannot be assigned to any specific protein (see Fig. SI4). To determine whether it is possible to assign specific protein peaks in a whole organism would require a statistical analysis that would take into account protein abundance, structure and amino acid chemical shift dispersion. Alternatively, a specific protein can be overexpressed or specific organelles in which a protein is largely dominant could be purified. This approach has been pioneered by Fu et al. (2011), and has benefited from recent progress in high-field magnets, fast spinning MAS probes, and the development of Dynamic Nuclear Polarization (Warnet et al. 2015; Renault et al. 2012).

We examined the possible presence of contamination products in the microalgal cell sample. In the dark and in the absence of an oxygen source, such as in the rotor during the experiment, *C. reinhardtii* could potentially be able to ferment carbohydrates producing formate, acetate, and ethanol (Catalanotti et al. 2013). No traces of these easily detectable products were observed in our spectra after up to 48 h of data acquisition.

In a complementary approach to ours—which relies on solution NMR methods—the group of Simpson has studied highly mobile soluble components in ^{13}C-labelled *C. reinhardtii* suspensions (Akhter et al. 2016). The authors successfully detected small metabolites, notably by exploiting the higher sensitivity of ^{1}H detection. Some of these metabolites could also be detected using high-resolution ^{13}C NMR although with greater difficulty (Akhter et al. 2016). Using diffusion-based filter-editing techniques, the authors were able to distinguish molecules according to their mobility. It is interesting to compare their RADE spectrum—which excite the most rigid molecules detectable by solution NMR—to our approach. The complementarity is striking, as the most rigid components detectable by solution-state NMR correspond to the most mobile components detectable by high-resolution solid-state NMR (see for example Fig. 1e). In our ^{13}C detected spectra, very fast diffusing molecules such as small metabolites are hard to detect, to the extent of becoming virtually absent.

Conclusion

In this work we demonstrated that despite the a priori huge complexity of fully ^{13}C-labelled microorganism, in vivo solid-state NMR can provide valuable information on the chemical nature and dynamics of cell constituents. Application of dynamical filters to high-resolution 2D solid-state NMR enabled the in situ identification of important constituents of *C. reinhardtii*. The major membrane lipids MGDG and DGDG were identified, along with carbon resonances on the fatty acyl chains. The galacto- and arabinofuranose carbohydrate which take part in the cell wall glycoprotein architecture were identified in different types of bondings. Also notably, the amylose in the starch storage grains was identified as crystallizing mainly in the A form. To further pursue the assignment of the various constituents, dynamic filtering could be combined to selective labelling. Furthermore, the study of isolated organelles or cell constituents such as the cell wall could assist a future full assignment within the whole cell. Assignment of molecule signals is the bottleneck of every NMR study. Once assigned, these signals can be followed in order to localize, within the cell, molecules that are affected by changes in the microorganism life-cycle. Such changes can be wanted, for example when overexpression of specific molecules is triggered, or not, for example when the cells are attacked by bacteria or polluting agents. This work thereby paves the way to the study of the effect of contaminants and bioengineering on microalgal cells in situ.

Acknowledgements The authors would like to thank Dr. Francesca Zito (CNRS, France) for providing the *Chlamydomonas* strain and her insights on *Chlamydomonas* growth and physiology. This work was supported by the Natural Sciences and Engineering Research Council (NSERC) of Canada (Grant 326750-2013 to I.M.) and the Centre National de la Recherche Scientifique (UMR 7099 to D.E.W.). J.-P.B. would like to acknowledge the Groupe de Recherche Axé sur la Structure des Protéines (GRASP) and the NSERC for the award of scholarships. B.G. would like to thank the Canadian Institutes of Health Research Strategic Training initiative in Chemical Biology and the Réseau Aquaculture Québec (RAQ) for the award of scholarships. IM and RT are members of the RAQ.

References

Akhter M et al (2016) Identification of aquatically available carbon from algae through solution-state NMR of whole (13)C-labelled cells. Anal Bioanal Chem 408:4357–4370

Andronesi OC et al (2005) Determination of membrane protein structure and dynamics by magic-angle-spinning solid-state NMR spectroscopy. J Am Chem Soc 127:12965–12974

Arnold AA et al (2015) Identification of lipid and saccharide constituents of whole microalgal cells by ^{13}C solid-state NMR. Biochim Biophys Acta 1848:369–377

Beal CM, Webber ME, Ruoff RS, Hebner RE (2010) Lipid analysis of Neochloris oleoabundans by liquid state NMR. Biotechnol Bioeng 106:573–583

Blaby IK et al (2014) The Chlamydomonas genome project: a decade on. Trends Plant Sci 19:672–680

Boender GJ, Raap J, Prytulla S, Oschkinat H, De Groot HJ (1995) MAS NMR structure refinement of uniformly ^{13}C enriched chlorophyll a/water aggregates with 2D dipolar correlation spectroscopy. Chem Phys Lett 237:502–508

Bollig K et al (2007) Structural analysis of linear hydroxyproline-bound O-glycans of *Chlamydomonas reinhardtii*—conservation of the inner core in Chlamydomonas and land plants. Carbohydr Res 342:2557–2566

Bonente G, Pippa S, Castellano S, Bassi R, Ballottari M (2012) Acclimation of *Chlamydomonas reinhardtii* to different growth irradiances. J Biol Chem 287:5833–5847

Boyle NR, Morgan JA (2009) Flux balance analysis of primary metabolism in *Chlamydomonas reinhardtii*. BMC Syst Biol 3:4

Bradbury JH, Jenkins GA (1984) Determination of the structures of trisaccharides by 13C-n.m.r. spectroscopy. Carbohydr Res 126:125–156

Buleon A et al (1997) Starches from A to C. *Chlamydomonas reinhardtii* as a model microbial system to investigate the biosynthesis of the plant amylopectin crystal. Plant Physiol 115:949–957

Catalanotti C, Yang W, Posewitz MC, Grossman AR (2013) Fermentation metabolism and its evolution in algae. Front Plant Sci 4:150

Dick-Perez M et al (2011) Structure and interactions of plant cell-wall polysaccharides by two- and three-dimensional magic-angle-spinning solid-state NMR. Biochemistry 50:989–1000

Ferris PJ et al (2001) Glycosylated polyproline II rods with kinks as a structural motif in plant hydroxyproline-rich glycoproteins. Biochemistry 40:2978–2987

Fu R et al (2011) In situ structural characterization of a recombinant protein in native *Escherichia coli* membranes with solid-state magic-angle-spinning NMR. J Am Chem Soc 133:12370–12373

Guschina IA, Harwood JL Algal lipids and effect of the environment on their biochemistry. In: Lipids in aquatic ecosystems (Arts MT, Brett MT, Kainz MJ (eds)) pp 1–24 (Springer, 2009)

Johns SR, Ralph Leslie D, Willing RI, Bishop DG (1977) Studies on chloroplast membranes. II ^{13}C chemical shifts and longitudinal relaxation times of 1,2-di[(9Z,12Z,15Z)-octadeca-9,12,15-trienoyl]-3-galactosyl-sn-glycerol. Aust J Chem 30:823–834

Johns SR, Ralph Leslie D, Willing RI, Bishop DG (1978) Studies on chloroplast membranes. III ^{13}C chemical shifts and longitudinal relaxation times of 1,2-diacyl-3-(6-sulpho-a-quinovosyl)-sn-glycerol. Aust J Chem 31:65–72

Kilz S, Waffenschmidt S, Budzikiewicz H (2000) Mass spectrometric analysis of hydroxyproline glycans. J Mass Spectrom 35:689–697

Merchant SS et al (2007) The Chlamydomonas genome reveals the evolution of key animal and plant functions. Science 318:245–250

Merchant SS, Kropat J, Liu B, Shaw J, Warakanont J (2012) TAG, you're it! Chlamydomonas as a reference organism for understanding algal triacylglycerol accumulation. Curr Opin Biotechnol 23:352–363

Renault M et al (2012) Cellular solid-state nuclear magnetic resonance spectroscopy. Proc Natl Acad Sci USA 109:4863–4868

Rondeau-Mouro C, Veronese G, Buleon A (2006) High-resolution solid-state NMR of B-type amylose. Biomacromol 7:2455–2460

Siaut M et al (2011) Oil accumulation in the model green alga *Chlamydomonas reinhardtii*: characterization, variability between common laboratory strains and relationship with starch reserves. BMC Biotechnol 11:7

Siemer AB et al (2006) Observation of highly flexible residues in amyloid fibrils of the HET-s prion. J Am Chem Soc 128:13224–13228

Specht E, Miyake-Stoner S, Mayfield S (2010) Micro-algae come of age as a platform for recombinant protein production. Biotechnol Lett 32:1373–1383

Tan L, Qiu F, Lamport DT, Kieliszewski MJ (2004) Structure of a hydroxyproline (Hyp)-arabinogalactan polysaccharide from repetitive Ala-Hyp expressed in transgenic *Nicotiana tabacum*. J Biol Chem 279:13156–13165

Tang H, Hills BP (2003) Use of ^{13}C MAS NMR to study domain structure and dynamics of polysaccharides in the native starch granules. Biomacromol 4:1269–1276

van den Hoek C, Mann DG, Jahns HM Algae: an introduction to phycology, (Cambridge University Press, Cambridge, 1995)

Vieler A, Wilhelm C, Goss R, Suss R, Schiller J (2007) The lipid composition of the unicellular green alga *Chlamydomonas reinhardtii* and the diatom *Cyclotella meneghiniana* investigated by MALDI-TOF MS and TLC. Chem Phys Lipids 150:143–155

Wang T, Hong M (2016) Solid-state NMR investigations of cellulose structure and interactions with matrix polysaccharides in plant primary cell walls. J Exp Bot 67:503–514

Warnet XL, Arnold AA, Marcotte I, Warschawski DE (2015) In-cell solid-state NMR: an emerging technique for the study of biological membranes. Biophys J 109:2461–2466

Warschawski DE, Devaux PF (2000) Polarization transfer in lipid membranes. J Magn Reson 145:367–372

Wijffels RH, Barbosa MJ (2010) An outlook on microalgal biofuels. Science 329:796–799

Supplementary Information for

Whole cell solid-state NMR study of *Chlamydomonas reinhardtii* microalgae.

Alexandre A. Arnold[†], *Jean-Philippe Bourgouin*[†], *Bertrand Genard*[§†], *Dror E. Warschawski*[†#], *Réjean Tremblay*[§] *and Isabelle Marcotte*[†*]

[†]Department of Chemistry, Université du Québec à Montréal, P.O. Box 8888, Downtown Station, Montreal, Canada, H3C 3P8

[§]Institut des Sciences de la Mer de Rimouski, Université du Québec à Rimouski, 310 allée des Ursulines, Rimouski, Canada G5L 3A1

[#]Laboratoire de Biologie Physico-Chimique des Protéines Membranaires, UMR 7099, CNRS, Université Paris Diderot and IBPC, 13 rue Pierre et Marie-Curie, 75005 Paris, France

*corresponding author : marcotte.isabelle@uqam.ca

+1 514 987 3000 ext. 5015

Detailed microalgal cells growth conditions

Chlamydomonas reinhardtii wild type strain 222+ was cultivated in a Minimum-Tris medium (Tris-phosphate with no acetate). The autoclaved medium was supplemented with $NaH^{13}CO_3$ to a final concentration of 0.1% (w/v). The carbonate was first dissolved in approximately 10% of the final volume of medium and then filtered using a 0.22 µm filter. The culture was inoculated by cells grown on petri dish of the same media with 1,5% agar. The large inoculum of thick textured was scrubbed on the glass wall to allow its dispersion in the media. The culture was then sealed and purged with filtered (0.22 µm) nitrogen to eliminate atmospheric CO_2. The culture was allowed to grow for 5 days under constant gentle shaking and a continuous illumination at an approximate photon flux of 100 µmol photons $m^{-2}s^{-1}$ (Sylvania GRO-LUX Wide Spectrum F40) at a temperature of 23^0C±1. Under these conditions, algae were thus harvested in the plateau region of the growth curve. The minimum Tris-phosphate (TP) medium supplemented with bicarbonate is composed of 20 mM Tris; 12 mM $NaH^{13}CO_3$; 7.5mM NH_4Cl; 0.81 mM Na_2HPO_4; 0.53 mM KH_2PO_4; 0.41 mM $MgSO_4•7H_2O$; 0.35 mM $CaCl_2•2H_2O$; 0.18 mM H_3BO_3; 0.15 mM EDTA•2Na; 77 µM $ZnSO_4•7H_2O$; 26 µM $MnCl_2•2H_2O$; 18 µM $FeSO_4•7H_2O$; 6.8 µM $CoCl_2•6H_2O$; 6.3 µM $CuSO_4•5H_2O$; 0.89 µM $(NH_4)6Mo_7O_{24}•4H_2O$. The pH of the medium prior to carbonate addition was 7.3±0.1.

Starch extractions

Cells were cultivated as described in the section above. We adapted the protocols of starch extraction from Buléon et al.. Cells were centrifuged 8 min at 1600g. Rinsed twice with 10mM Tris HCl at pH 8, then re-centrifuged. Cells were diluted with the same

buffer at a concentration of 10^8 cell/ml and then lysed by a sonication probe in an ice bath for 3 cycles of 30 seconds separated by cooling cycles to avoid excessive heating. The lysate was centrifuged 15 min at 2000g at 5°C. The supernatant was removed and the pellet re-suspended into one volume of buffer for another cycle of sonication, then re-centrifuged into the same conditions. The supernatant was removed and the pellet re-suspended in one volume of buffer and added gently to avoid mixing on 5 volumes of Percoll (colloidal silica particles of 15-30 nm diameter coated with PVP) and centrifuged again. The pellet was again re-suspended in one volume of buffer then passed through another 5 volumes of Percoll solution. The pellet was rinsed twice with milli-q water at 4°C and freeze-dryed.

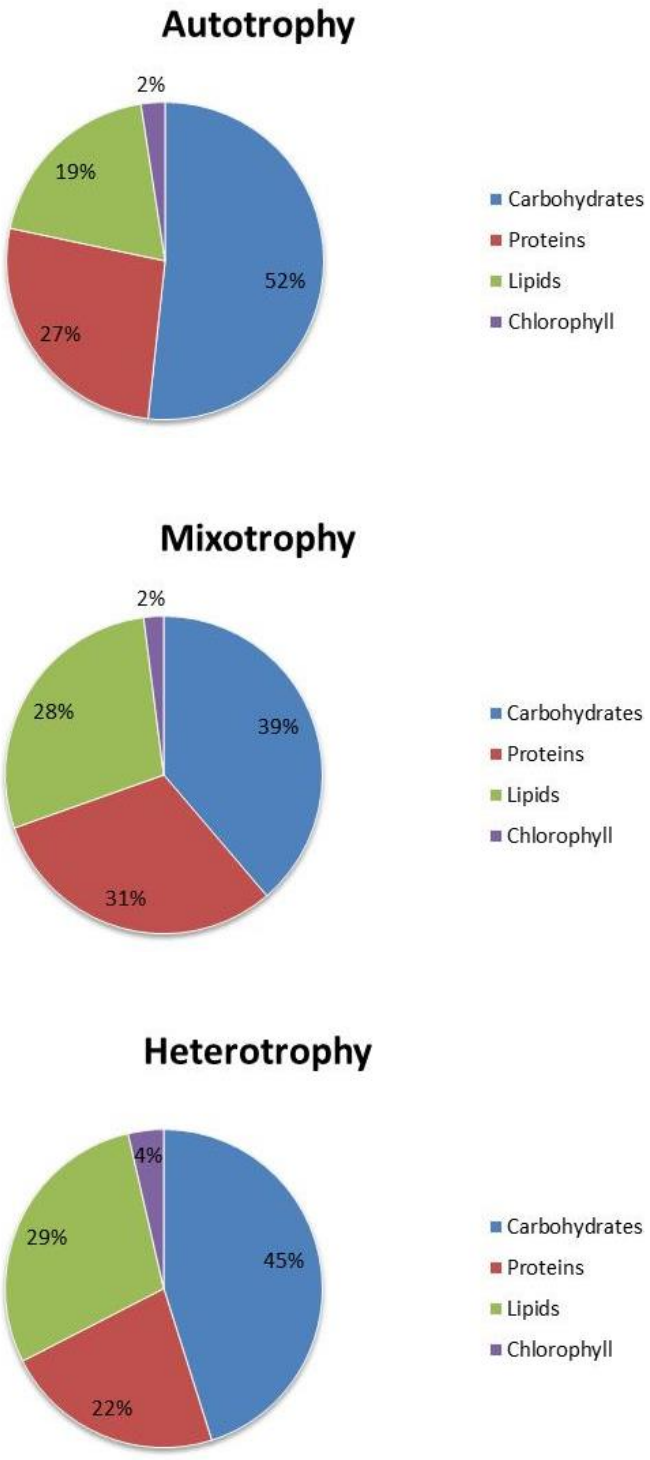

Figure SI1. Relative proportions of cell components of *Chlamydomonas reinhardtii* grown under various conditions. Adapted from Boyle and Morgan[1].

Polar lipids

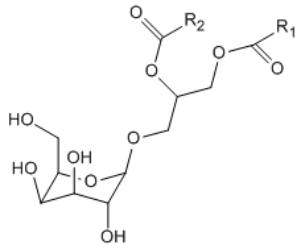

monogalactosyl diacylglyceride (MGDG 38%)

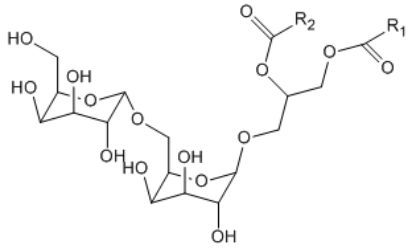

digalactosyl diacylglyceride (DGDG 24%)

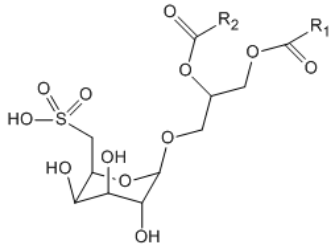

sulfoquinovosyl diacylglycerol (SQDG 12%

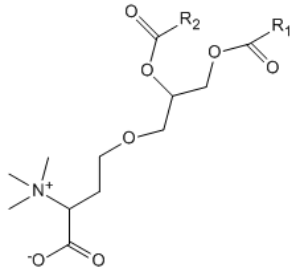

diacylglyceryl-trimethylhomoserine (DGTS 12%)

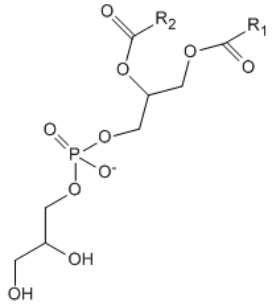

phosphatidylglycerol (PG 10%)

Apolar storage lipid

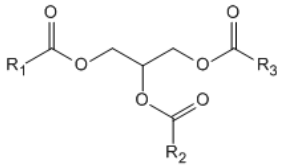

Triglyceryl oleate (triacylglycerol)

Main pigment

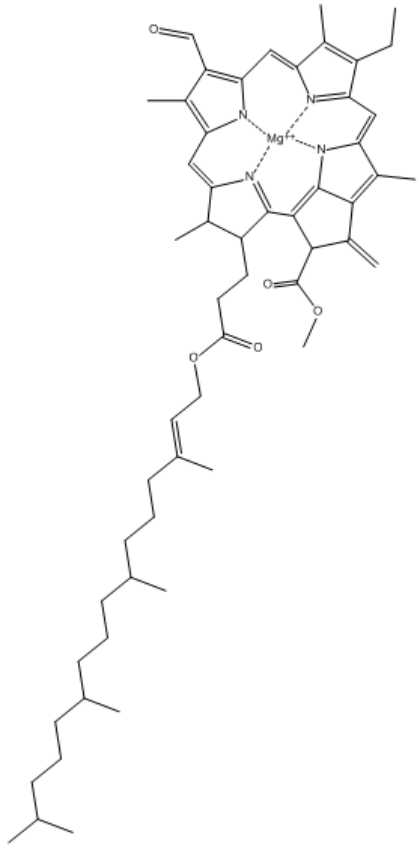

Chlorophyll-a

Figure SI2. Structures and relative abundances of the main lipids and pigments of *Chlamydomonas reinhardtii*[2].

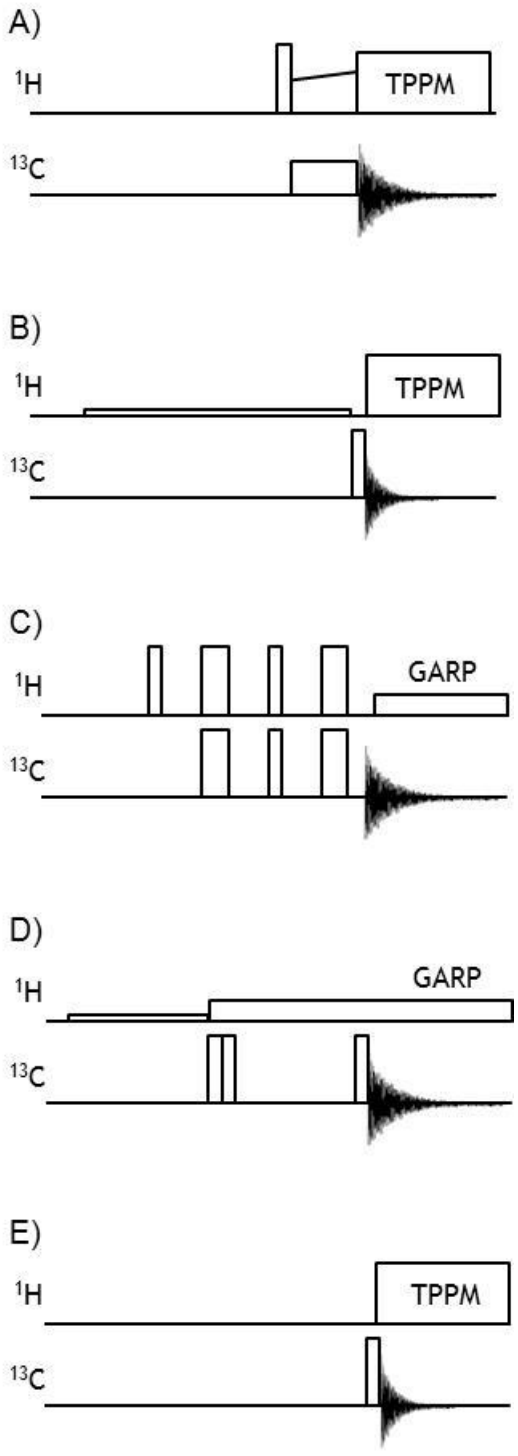

Figure SI3. One dimensional pulse schemes used for dynamical selectivity using a single polarization step. A) Cross-polarization, B) NOE, C) Refocused INEPT (RINEPT), D) NOE with ^{13}C T_1 filter and E) Direct excitation.

Table SI1. ^{13}C chemical shift literature values of most abundant lipids in *C. reinhardtii* and assigned experimental values (shown in italic between parentheses).

.

Assignment	MGDG[3]	DGDG[3]	SQDG[4]	DGTS[5]	TAG[6]
C1 C1'	104.8 *(103.2)*	104.7*(103.2)* 100.1 (*100.2)*	100.1	-	-
C2 C2'	71.9 *(71.1)*	71.9 *(71.1)* 70.6 *(70.3)*	73.4	-	-
C3 C3'	74.3 *(73.5)*	74.7 *(73.5)* 70.1	74.9	-	-
C4 C4'	69.8 *(70.2)*	69.7 *(70.2)* 70.3	74.9	-	-
C5 C5'	76.1 *(76.5)*	74.1 *(74.0)* 71.2	71.7	-	-
C6 C6'	61.9 *(61.8)*	67.3 *(68.1)* 62.3	54.3	-	-
Glyc-3 Glyc-2 Glyc-1	68.3 *(67.5)* 71.3 *(71.5)* 63.7 *(63.3)*	68.3 *(67.5)* 71.9 *(71.5)* 63.6 *(63.3)*	69.7 72.3 64.2	69.7 70.0 62.3	68.9 62.1 68.9
$(CH_3)_3N^+$	-	-	-	52.3	-
COO^-	-	-	-	176.7	-
-O-CH2-	-	-	-	67.9	-
C=O (sn-1) C=O (sn-2)	173.9 174.2	173.8 174.2	174.7 174.9	171.1 171.5	173.1 172.8
2	34.6	34.6		34.2	33.8
3	25.6	25.6			24.9
4-6	29.9	29.9			29.4
H2C*-H2C-CH=CH-	30.4	30.4			
CH2-C*H2-CH=CH	27.8	27.8			
CH2-CH2-C*H=CH	130.6-132.3	130.6-132.3		128-130	130.2
=CH-C*H2-CH=	26.2 *(26.0)*	26.2 *(26.0)*		25.7	
=CH-CH2-C*H=C*H-CH2-CH=	128.8 *(128.0)*	128.8 *(128.0)*			
C*H2-CH3	21.1 *(21.1-23.4)*	21.1 *(21.1-23.4)*			27.2
C*H3	14.6 *(14.5-14.8)*	14.6 *(14.5-14.8)*		14.1	14.1

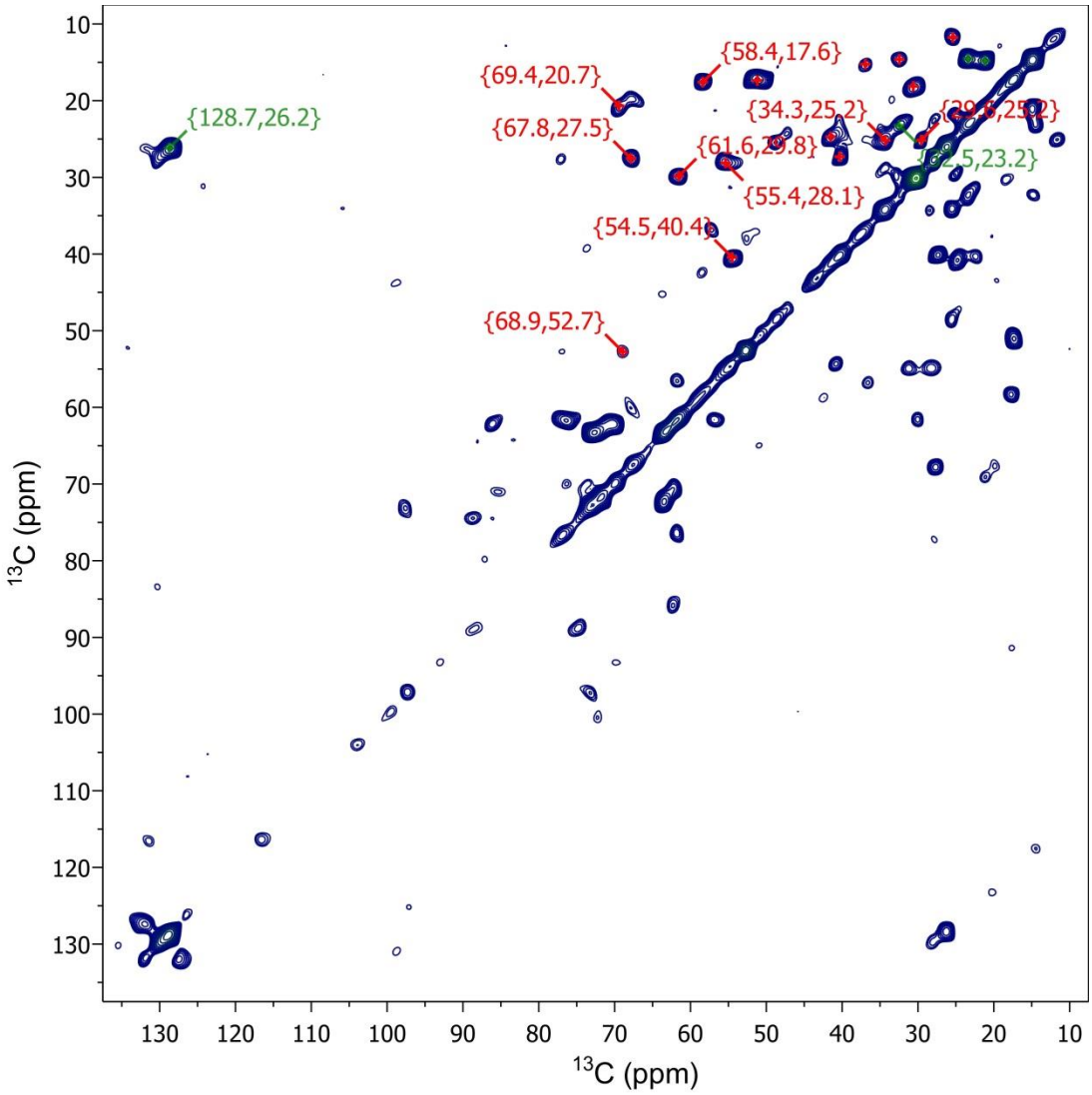

Figure SI4. Complete ^{13}C RINEPT-TOBSY spectrum showing the crowded aliphatic region between 0 and 50 ppm. The peak positions in green are those tentatively assigned to lipid peaks while those in red correspond to various amino acid peaks.

References

1. Boyle, N.R. & Morgan, J.A. Flux balance analysis of primary metabolism in Chlamydomonas reinhardtii. *BMC Syst. Biol.* 3, 4 (2009).

2. Vieler, A., Wilhelm, C., Goss, R., Suss, R. & Schiller, J. The lipid composition of the unicellular green alga Chlamydomonas reinhardtii and the diatom Cyclotella meneghiniana investigated by MALDI-TOF MS and TLC. *Chem. Phys. Lipids* 150, 143-55 (2007).

3. Johns, S.R., Ralph Leslie, D., Willing, R.I. & Bishop, D.G. Studies on chloroplast membranes. II 13C chemical shifts and longitudinal relaxation times of 1,2-di[(9Z,12Z,15Z)-octadeca-9,12,15-trienoyl]-3-galactosyl-sn-glycerol. *Aust. J. Chem.* 30, 823-834 (1977).

4. Johns, S.R., Ralph Leslie, D., Willing, R.I. & Bishop, D.G. Studies on chloroplast membranes. III 13C chemical shifts and longitudinal relaxation times of 1,2-diacyl-3-(6-sulpho-a-quinovosyl)-sn-glycerol. *Aust. J. Chem.* 31, 65-72 (1978).

5. Evans, R.W., Kates, M. & Wood, G.W. Identification of diacylglycerol-O-(N, N,N-trimethyl)-homoserine in the halotolerant alga, Dunalielle parva. *Chem. Phys. Lipids* 31, 331-338 (1982).

6. Beal, C.M., Webber, M.E., Ruoff, R.S. & Hebner, R.E. Lipid analysis of Neochloris oleoabundans by liquid state NMR. *Biotechnol. Bioeng.* 106, 573-583 (2010).